A ROTATIONAL INERTIAL CLOCK FOR GRAVITATIONAL REDSHIFT COMPARISONS

CARL H. LEYH, W. STEPHEN CHEUNG, BRUCE E. BERNARD, AND ROGERS C. RITTER

DEPARTMENT OF PHYSICS, UNIVERSITY OF VIRGINIA
CHARLOTTESVILLE, VIRGINIA 22901 U.S.A.

in

Proceedings of the 1983 International School and Symposium on Precision Measurement and Gravity Experiment, Taipei, Republic of China, January 24 - February 2, 1983, ed. by W.-T. Ni (Published by National Tsing Hua University, Hsinchu, Taiwan, Republic of China, June, 1983)

OUTLINE

A ROTATIONAL INERTIAL CLOCK FOR GRAVITATIONAL REDSHIFT COMPARISONS*

Carl H. Leyh, W. Stephen Cheung,** Bruce E. Bernard, and Rogers C. Ritter

Department of Physics, University of Virginia
Charlottesville, VA 22901 U.S.A.

I. Introduction

In the past precision macroscopic rotors have rarely been used in experiments to determine the nature or properties of gravity. While the general advantages and limitations of "corotation" rotor systems are explored in another paper presented at this conference[1], this paper will explore an application of one such system. That is, a precision macroscopic rotor is to be used as a rotational inertial clock for gravitational redshift comparisons.

It is conceivable, if there is a non-metric coupling between gravitational and electromagnetic forces, that a difference in gravitational redshift measurements could be observed in a comparison of clocks that have differing electromagnetic properties.[2] This difference in the gravitational redshift can be expressed in the THεμ formalism expansion[3] shown in Table I.[4]

The experiment would be to compare different clocks at a point on the earth's surface that move a "vertical" distance, h, from noon to midnight in the sun's gravitational potential. This means that the largest term is $gh/c^2 \approx 8 \times 10^{-13}$.

Hence, the clocks for this experiment must have a precision and stability of $\sim 10^{-15}$. The hydrogen maser and the superconducting cavity stabilized oscillator (SCSO) have under some conditions, this level of stability and precision, and have been compared in this kind of experiment with, as yet, inconclusive results.[5] A third clock would provide redundant information that could help distinguish between the daily gravitational redshift and other local disturbances that also have a diurnal variation.

There are many disturbances[6] that affect rotor stability and create drag. The two most important drag mechanisms are bearing friction and gas drag. To overcome the problem of gas drag, an old idea of Beam's[7] has been resurrected. This idea is to use an outer, corotating chamber with the inertial rotor. With the chamber evacuated to the molecular flow regime (e.g. 10^{-5} torr), the residual gas will corotate with the system, thereby virtually eliminating the gas drag effect. This scheme is needed since a decay time (1/e of the original ω) of 10^{15} sec. which is required for this experiment, would for a rotor in a non-corotating system require an unachievable vacuum of 10^{-14} torr.

Bearing drag is overcome by using a unique double magnetic suspension system, the details of which are discussed in another paper

presented at this conference.[8] This paper will be limited to a discussion of the corotation mechanism that is used in this first, room-temperature inertial clock.

II. The Servo Controlled Corotation System

The servo control system has four main components: (a) the two rotors, (b) the optical timing system, (c) the torque drive mechanism, and (d) the microcomputer control and data acquisition system. Only a brief description of components (a), (b), and (c) will be given while (d) will be discussed in detail.

(a) Rotors

The two rotors are designated as the shroud rotor and the proof rotor. The shroud rotor is magnetically suspended inside a vacuum chamber, and the proof rotor is magnetically suspended below and within the shroud rotor. The shroud rotor consists of a magnetic support slug attached to a tube containing 5 cylindrical rare earth magnets 0.6 cm. long and 1.25 cm. in dia. These magnets are used to suspend the proof rotor. Attached to this tube is a cylindrical lucite, "shroud" chamber of length 5.7 cm., OD 4.7 cm., and ID 4.3 cm. in which the proof rotor is suspended. Previous experience[9,10] has taught us that asymmetries in the magnetic field of the proof rotor suspension will produce a coupling torque between the proof and shroud rotors. In order to minimize any asymmetry due to a misalignment of the 5 support magnets, the magnets have been machined to a diameter tolerance of <0.002 mm and their holding tube has been constructed to the same tolerance.

The proof rotor is made of ferrite and is cylindrical in shape with a length of 3.8 cm and a dia. of 1.3 cm. A nylon ring is press fitted about the ferrite cylinder and on it a mirrored surface is formed. A mirrored surface is also formed on the shroud rotor.

Due to the laborious precision machining needed to minimize geometric asymmetries in the rotors, the new rotors were still under construction at the time of this writing. Hence the final mass and moment of inertia of the rotors, are not known at present. However, the expected moments of inertia are ~ 200 gm-cm^2 for the shroud rotor and ~ 20 gm-cm^2 for the proof rotor.

(b) Optical Timing System

The periods and relative position of the rotors are determined by counters which are controlled by the microcomputer and are connected to an external 1 MHz crystal oscillator. These counters are actuated by TTL pulses that originate in the optical timing system.

The light source is a 3 mW laser whose beam is split and brought to the vacuum chamber by two optical fibers. The optical fibers can be easily secured to the vacuum chamber to prevent any relative motion between the experiment and the light source, due to vibrations, that might be interpreted as a rotor fluctuation.

The light beams emerging from the fibers are focussed on to the rotors mirrored surfaces and are reflected into two respective split photodiodes. The two rotor photodetectors are of the same design. The split photodiode halves are tied together in a differential amplifier configuration. As the light beam is reflected off the rotating mirrored surfaces, it is swept across the photodiode which then produces a zero crossing signal at the output of the differential amplifier. A conventional zero-crossing detector with hysterisis shapes the pulse for a 74LS14 Schmidt trigger which provides a TTL compatable signal that is then sent through a 74LS244 Line Driver to the digital counters.

A bench test set up of this system showed a timing fluctuation of $< 10^{-6}$.

(c) Torque Drive Mechanism

The corotation of the shroud rotor with the proof rotor is achieved by speeding up or slowing down the shroud rotor so that it follows the proof rotor. This "motor" is an eddy current drive which uses two orthogonal pairs of coils through which an ~ 2.7 kHz sine wave current signal is sent in quadrature.[10] This technique is well known and will not be explained here.[9]

The amplitude of the torque drive is set by a variable resistor so that the feedback control torque is constant when applied. However, the feedback servo control determines the direction and the length of time the torque is applied and thereby controls the shroud rotor by a torque pulse width modulation.

The torque drive can operate in two modes: (1) The atmospheric, and (2) the vacuum mode. In the atmospheric mode the system is operated at atmospheric pressure, in which case an off-set torque must be applied to keep the shroud rotor from slowing down. The feedback torque signal, then, simply adds to or subtracts from the off-set torque. The subtraction is accomplished by a 180° phase shift of the feedback torque with respect to the off-set torque. In the vacuum mode there is 10^{-3} smaller off-set torque. The addition of the feedback torque can be accomplished in the same manner as in the first mode, but the subtraction cannot be the same. In this mode only the cosine position of the eddy current drive signal is given a 180° phase shift. This, in effect, causes the eddy current drive to reverse itself.

Hence, in either mode, the shroud rotor angular velocity can be controlled by varying the length of time and direction of the torque applied to the shroud rotor.

(d) Microcomputer Control and Data Acquisition System

Two microcomputers are used for servo control and data acquisition purposes. The Nibbler microcomputer based on the National Semiconductor SC/MP II microprocessor chip, has a 4K ROM Basic interpreter and 28 K on board RAM. It was designed for industrial process control applications and is easily interfaced with peripheral boards via its address and data buses. The Nibbler handles all control functions and acquires the

raw data from the experiment. A Hewlett-Packard HP-87 Personal Computer is used for data acquisition from the Nibbler and long term data storage on its associated disc drive system.

The rotor period and relative position information is obtained from counter boards made of 74LS161 Binary Counter chips and either 74LS173 4-bit Memory Latches or 74LS374 Octal Edge Triggered D-type Flip-Flops. These boards are configured as 24-bit "words" with a maximum count value of $2^{23}-1$, and are clocked by an external 1 MHz crystal oscillator which has a stability of $< 10^{-6}$. Each 8-bit digit of the counter boards has its own position in the memory map of the Nibbler and hence is easily accessed by the control routine. (Ultimately the 1 MHz signal must be derived from the rotational period for this clock to generate its own time base.)

The servo control program is designed about the reception of a position signal from the experiment. Once this is obtained derivative and integrating functions can be performed as part of the feedback loop. This digital "signal" is a count value, N_S, obtained from a counter board that is turned on by a TTL signal from the shroud rotor optical system and then turned off by the proof rotor optical system. If both rotors have the same angular velocity, the recorded count (time) measures the angle between the mirrored surfaces. This is shown schematically in Fig. 1. The proof rotor period count, Np, defines an angle of 2π.

This count value, N_S, is compared with a reference angle that is set as an initial condition and can be changed. The resulting ΔN is the linear "control" signal that the servo-signal is attempting to drive to zero. When ΔN is subtracted from the previous sampling's ΔN, the result is a measure of how fast ΔN is being driven to zero, and hence is a velocity or derivative signal. When ΔN is added to all the previous sampling ΔN's, the result is an integrating of the "control" signal.

These three branches, linear, derivative and integral, can be given various weights by the program as shown in the block diagram of Figure 2. They are added together to produce the torque parameter, TP, which can also be adjusted by the program.

The servo control routine is so constructed that a negative torque parameter will produce a negative feedback torque on the shroud rotor and vice versa. The torque is applied to the shroud as long as there is a non-zero TP. The program decrements the TP count by one then tests for a zero TP and continues this loop until zero is reached. A torque cutoff time of ~ 0.2 sec. has been built into the program, and the shortest torque duration is, in principle, 60 μsec. (With an eddy current drive using ~ 2.7 kHz the shortest effective torque duration is ~ 400 μsec.)

Since the entire servo control routine is written in machine language it only takes ~ 5 msec to acquire the data and determine the TP. Transferring the data to the HP-87, however, is another matter. The HP-87 and the Nibbler communicate through a serial interface. The Nibbler was designed to operate in slow industrial environments and was originally programmed to transfer data at 110 baud. Through considerable effort the ROM program was changed to allow operation at

1175 baud. At this speed the HP-87 acts, with considerable programming tricks, as a terminal for the Nibbler, and the programming speed of the Nibbler has been greatly increased. Since the HP-87 can be programmed to recognize binary data streams (as opposed to the normal ASCII stream) the Nibbler can send data to the HP-87 without using the slow ROM Basic interpreter. The HP-87, however, must accept this data and reduce it for storage using its own Basic language program. While the HP Basic is faster than the Nibbler Basic it is still slow when compared with the Nibbler machine language and currently restricts the experiment to rotor periods no less than 0.5 sec in length.

Although the basic servo control routine was developed ~ 10 months ago, the acquisition of the HP-87 and its disc drive system has been relatively recent. Much time was needed to develope and debug the hardware and the software necessary to interface the Nibbler with the HP-87, and hence it is only now going into the testing stage.

III. Preliminary Results of the Servo Control System

The servo control routine was tested using the slow 110 baud rate data transfer system. Due to the slow data transfer rate, the test could not be made completely in real time. The results, however, were encouraging.

The test consisted of simulating the proof rotor with pulses from a function generator and then servoing the shroud rotor to this period. Figures 3 and 4 show the result of one such test. Performed at atmospheric pressure this test used a feedback torque amplitude of 0.5 dyne-cm with an off-set torque of 2.0 dyne-cm. The function generator period was adjusted to match that of the equilibrium period of the shroud rotor driven by the off-set torque. The □ show the simulated proof period and the + show the relative position of the shroud with respect to the "proof" rotor.

As is apparent from the figures the shroud rotor was moving past the "proof" rotor until it "locked in" and then it quickly approached the reference position with little hunting or overshoot. This test used a derivative weighting factor of unity, a linear weighting of unity and zero integral weight. Since with the counting system at the time the data was not recorded in real time, no value could be determined for the effective torsional "spring constant" or the effective torsional "damping coefficient".

Figure 4 shows how close the position of the shroud with respect to the reference position was controlled (to within 2 degrees). It is assumed that the reason that the shroud position did not straddle the zero position angle is that there is a non-zero servo error due to limited loop gain. Furthermore, this would be amplified if the off-set torque was not completely adjusted to produce an equilibrium period for the shroud rotor, given the gas drag at that speed, equal to that of the function generator.

In comparison, Fig. 5 shows the result of shroud and proof rotor periods when servoed with only derivative feedback.[10] The two rotors periods passed each other and then only slowly approached each other.

The oscillations produced on the proof rotor are presumed to have been caused by a magnetic torsional coupling between the rotors which, no doubt, was position dependent.

IV. Discussion of the Preliminary Results

The relationship of rotor angular velocity, ω, to the gas drag torque in a non-corotating system is well known.[10,11] For a non-corotating rotor system operating in the molecular flow regime, the relationship is expressed as,

$$L = -P\omega\sqrt{\frac{M}{2\pi kT}} \int_S r^2 dA, \qquad (1)$$

where P is the pressure of the vacuum, M is the mass of the residual gas molecules, k is Boltzman's constant, T is the absolute temperature and r is the radius variable of the rotor which is integrated over the surface area of the rotor. It is obvious from eqn. (1) that a reduction in the torque due to a smaller ω would be equivalent to a reduced effective P of a higher ω system. In a partially corotating gas atmosphere ω becomes the relative velocity between the rotor and the gas some distance from it. This has been tested.[12]

The test shown in Fig. 4 was not recorded in real time, but it is estimated that the 1° position fluctuation occurred over ~ 100 seconds. This would yield a relative angular velocity between the shroud and "proof" rotors of $\omega \approx 5$ rad/s. Hence a reduction in the relative ω from 5 rad/s to 10^{-4} rad/s would reduce the gas drag torque with the equivalent of ~ 10^{-4} pressure reduction in a non-corotating system with $\omega \approx 5$ rad/s.

Assuming that a corotating system operates in a vacuum of 10^{-5} torr, this amount of control would yield an effective pressure of 10^{-9} torr. An effective pressure of that value would be expected to yield a decay time constant of $\tau^* \approx 10^9$ to 10^{10} sec, if there are no other drag mechanisms present at this level of sensitivity.

It is anticipated that the improved system will control ω to 10^{-6} rad/sec, which if operated at a pressure of 10^{-8} torr, would in principle yield a τ^* of 10^{14} to 10^{15} sec. Although this is the ultimate goal for the inertial clock, it is expected that other drag mechanisms will appear at this level of speed constancy and these will require a considerable effort to successfully overcome them.

V. Conclusion

A microcomputer commanded corotation system is in development for use in an inertial clock experiment. The servo control algorithm incorporates derivative, linear, and integral feedback paths and in its very first operations has demonstrated limited controlling ability in tests at stmospheric pressure.

Changes for drastic improvement are in fabrication. Improvements have been made of the original rotor, optical sensing, and torque drive designs. Considerable increase has been achieved in data acquisition capability and ease, permitting higher inertial rotor frequencies, and facilitating the collection of large amounts of data

A first goal of 10^{-9} period stability has been reasoned from design criteria and past experiments, and serious pursuit of this is at hand.

*This research was supported in part by NSF Grant PHY80-07948 and NBS Grant G8-9025.

**Present address: Hanson Laboratories, Stanford University, Palo Alto, CA 94305 U.S.A.

REFERENCES

1. W. S. Cheung and R. C. Ritter, "Precision Rotors for Gravitation Experiments", in proceedings this symposium.

2. C. M. Will, General Relativity: An Einstein Centenary Survey. ed. S. W. Hawking and W. Israel. Cambridge Univ. Press (1979).

3. A. P. Lightman and D. L. Lee, Phys. Rev. D8, 3293 (1973).

4. C. M. Will, Private Communication.

5. S. R. Stein and J. P. Turneaure, AIP Conf. Proc. 44, 192 (1978).

6. G. R. Jones, Jr., R. C. Ritter, and G. T. Gillies, Metrologia, 18, 209 (1982).

7. J. W. Beams, Rev. Sci. Instrum. 34, 1071 (1963).

8. B. E. Bernard, W. S. Cheung, and R. C. Ritter, "Properties of a Double Magnetic Suspension", proceedings this symposium.

9. G. R. Jones, Jr., "Decay Time Studies of Magnetically Suspended Rotors", M. Sc. Thesis, University of Virginia, 1981.

10. W. S. Cheung, "Servo Driven Corotation: Development of an Inertial Clock", Doctoral Dissertation, Univ. of Virginia, 1982.

11. J. W. Beams, et al, Rev. Sci. Instrum. 33, 151 (1962).

12. G. R. Jones, Jr., "Developement of Precision Rotor Experiment for Matter Creation Test", Doctoral Dissertation, Univ. of Virginia, 1983.

Table I

Aspect of EM	Examples	Redshift in THεμ
Electrostatic Interactions	Principle lines of H Oscillations of High Q crystals Rotor Clock	$z = (1-2\Gamma_o)gh/c^2$
Hyperfine Interactions	H-Maser	$z = (1-3\Gamma_o+\Lambda_o)gh/c^2$
Electrostatic & light propagation	SCSO	$z = (1 - \frac{3}{2}\Gamma_o - \frac{1}{2}\Lambda_o)gh/c^2$

Where $z = \frac{\Delta\nu}{\nu}$

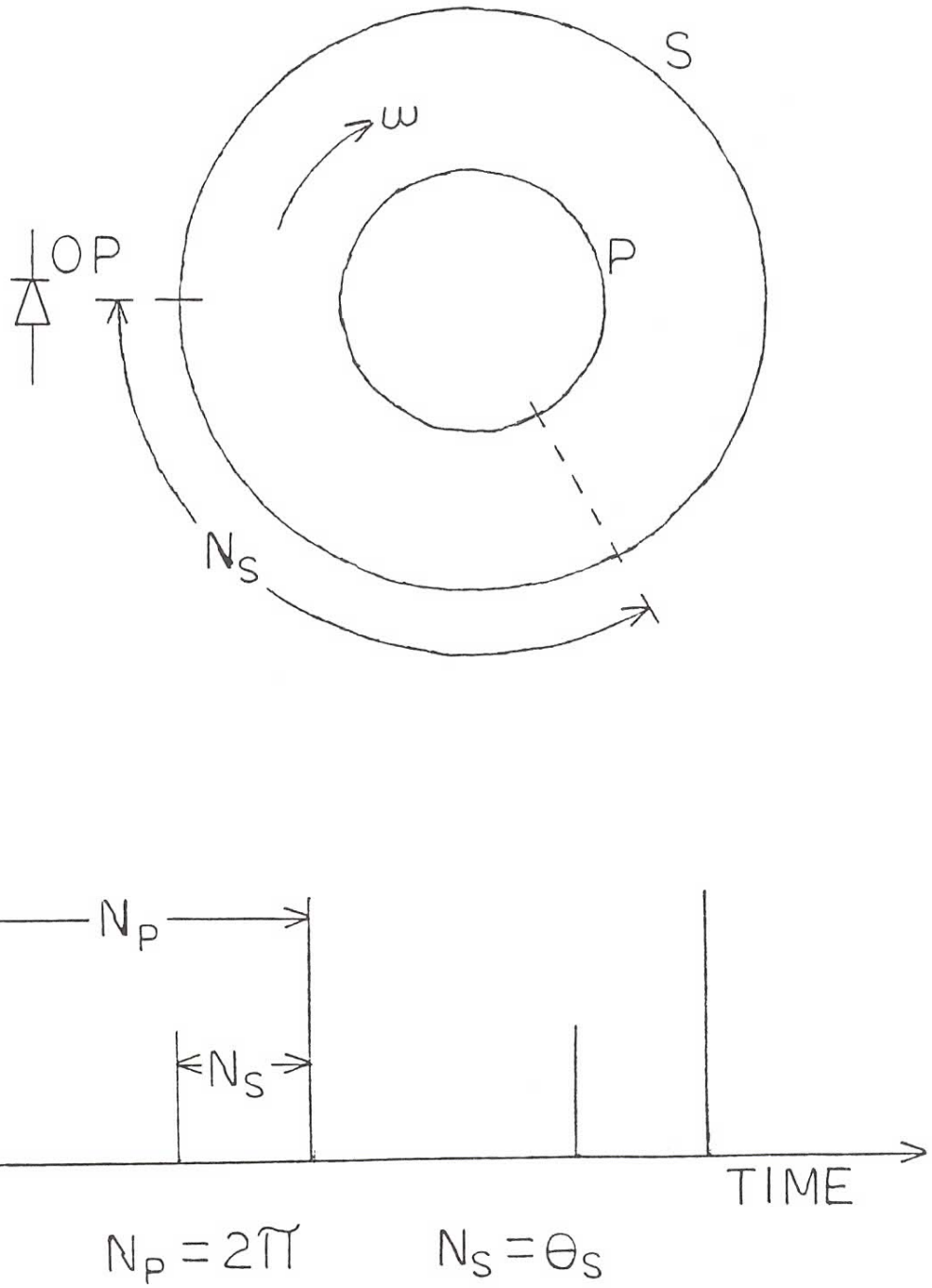

Fig. 1 Position-to-Count Schematic Diagram - The relative position of the shroud, s, to the proof, p, rotor is defined in counts, N_S, by the optical system, OP, starting a counter with a shroud pulse and stopping the counter with a proof pulse. The number of counts between successive proof pulses, N_p, define an angle of 2π. The lower figure shows the pulse sequence.

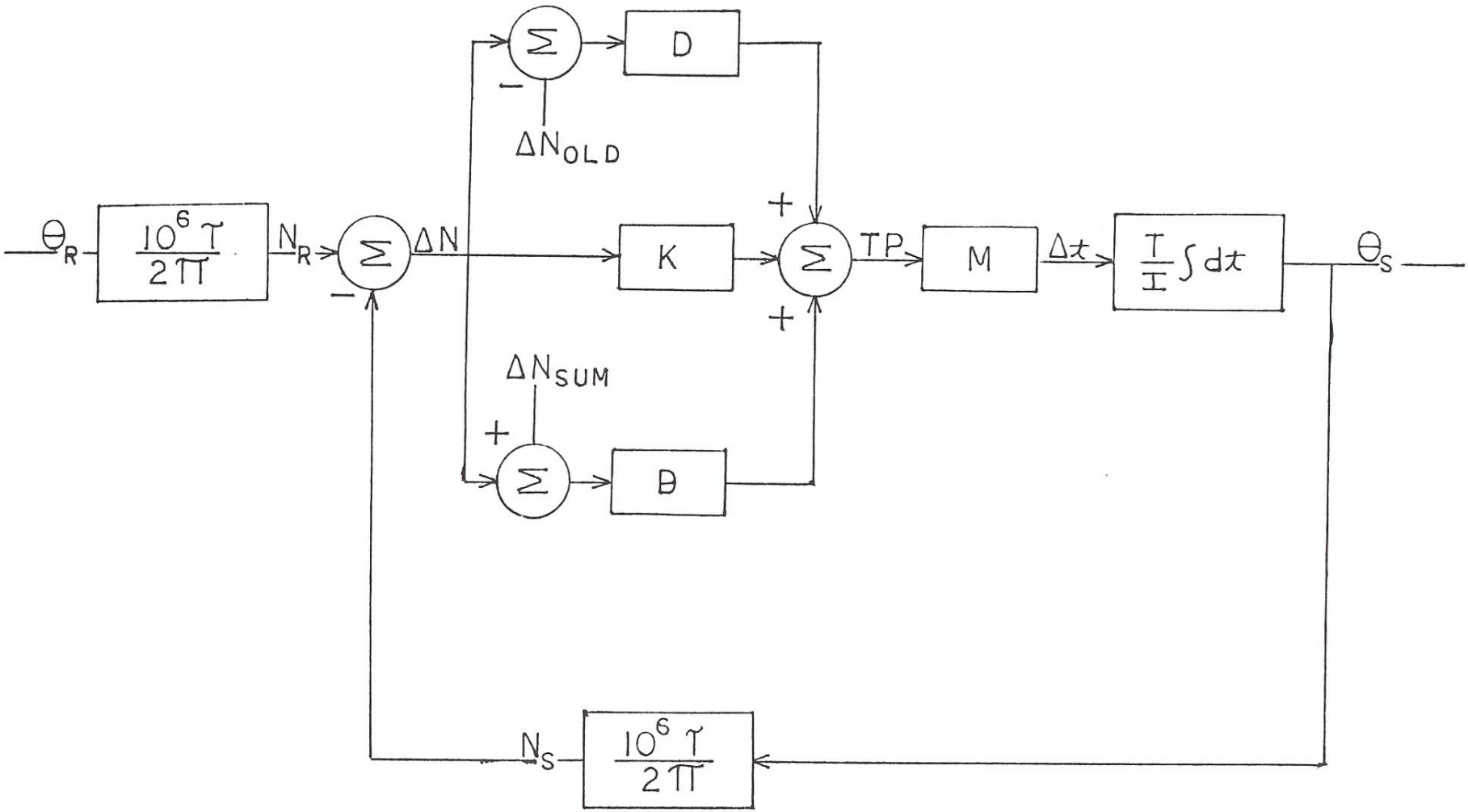

Fig. 2. Servo Control Feedback Scheme - The reference position, θ_R, is converted to counts, N_R, and mixed with the shroud position θ_S which has already been converted to counts N_S, where τ is the proof rotor period and is considered a constant. The control signal, ΔN, goes through three branches. These are multiplied by the weighting factors D, K, B for derivative, linear, and integral feedback, respectively. The sum of these three produce the torque parameter, TP, which opens the torque gate, and is converted to a time, Δt, by M. The time operates on the torque amplitude, T, to produce a change in angular momentum which is integrated by the rotor over time dt to produce a new shroud position θ_S.

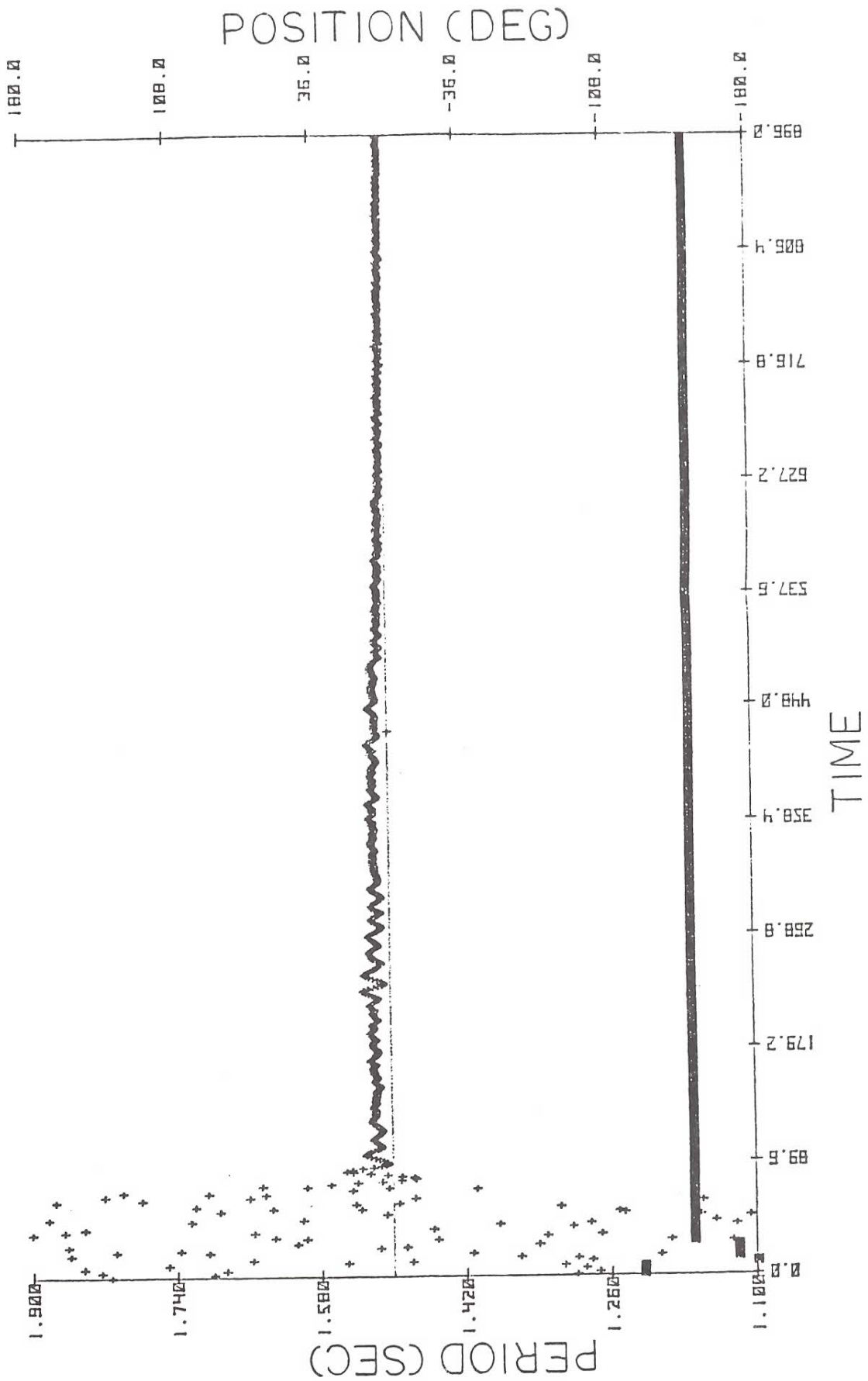

Fig. 3 System Simulated Test with Shroud Rotor Alone and With Derivative and Proportional Feedback - + shows the shroud position with respect to the reference position. □ shows the period of the function generator simulating the proof rotor. Starting with the shroud and "proof" rotors out of synchrony, the shroud is locked to the "proof" and rapidly converges to the reference position. Feedback torque ≈ 0.5 dyne-cm, offset torque ≈ 2.0 dyne-cm, derivative and linear weighting factors are equal. Time scale is in arbitrary units. The experiment was carried out under atmospheric pressure.

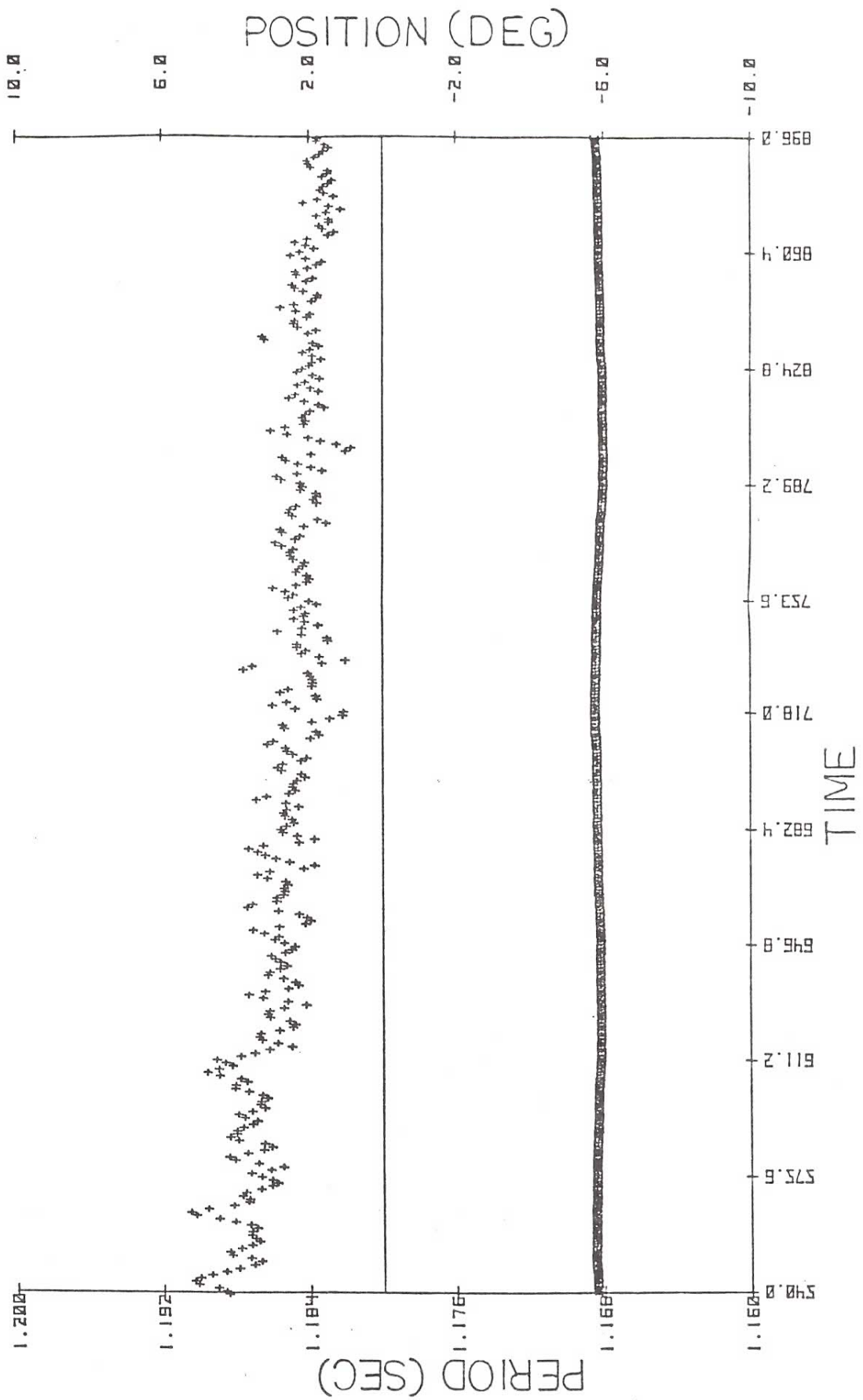

Fig. 4. Expansion of Fig. 3 - same conditions as in Fig. 3, but showing the detail of approach to finer control. Notice that the shroud position is held to within 2° and the position fluctuation at the end is < 1°. The approach to 0° is partly due to a periodic increase in the feedback torque to 2.0 dyne-cm. The position off-set is due to the fact that at the velocity set by the function generator frequency, the difference in driving and drag torques could not be overcome by the servo loop.

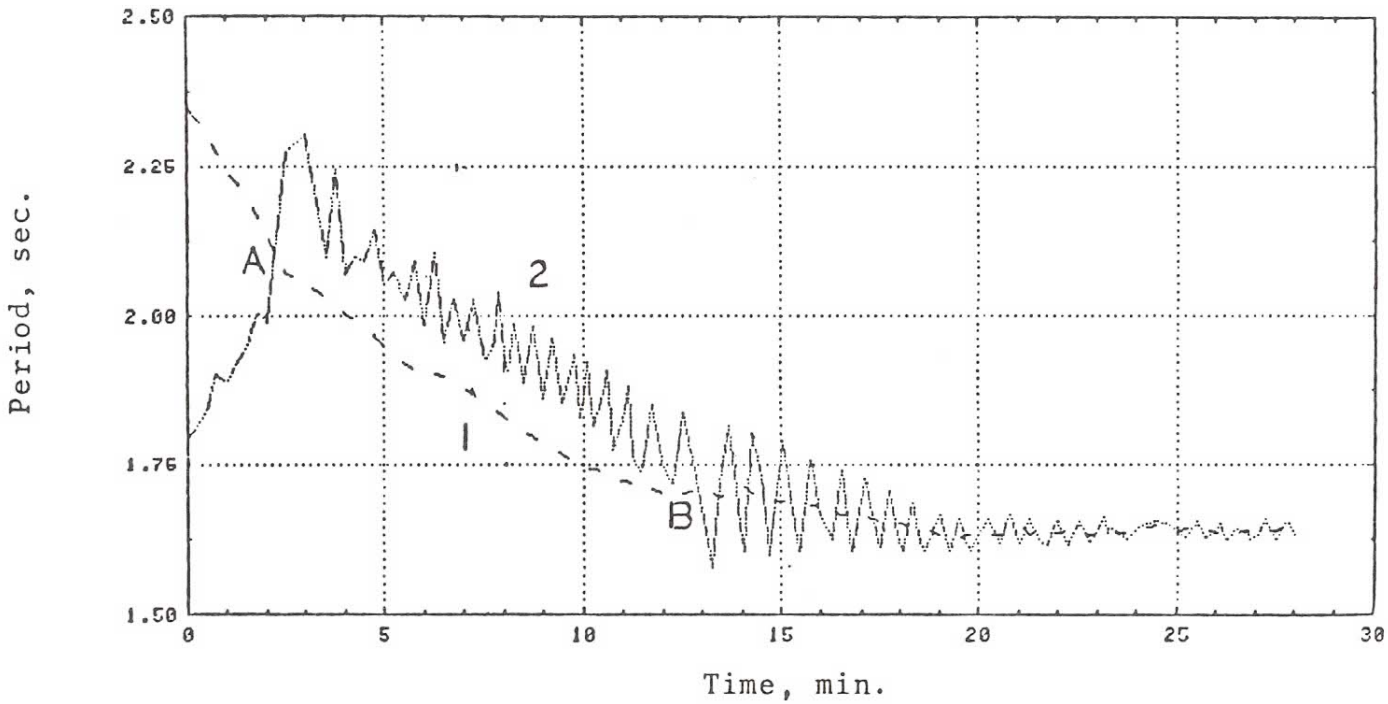

Fig. 5 Two-rotor Test With Derivative Feedback Alone - curve 1 is the shroud rotor and curve 2 is the true proof rotor. Although the curves cross at A the derivative feedback is not enough to "lock" the shroud to the proof rotor. The oscillation of the proof rotor is due to a magnetic torsional coupling between the rotors. Notice also the increase in the oscillation amplitude at B when the rotors lock together. The position-dependent torsional coupling helped pull the rotors together.